

Ultraviolet Lasing Phenomenon of Zinc Oxide Hexagonal Microtubes

Clement YUEN, Siu F. YU*, Xiao W. SUN, Chun X. XU, Eunice S. P. LEONG, Shu P. LAU and Chung K. CHEN

School of Electrical & Electronic Engineering, Nanyang Technological University, Block S2, Nanyang Avenue, Singapore 639798

(Received March 1, 2004; accepted April 9, 2004; published August 10, 2004)

Prismatic zinc oxide (ZnO) hexagonal microtubes have been fabricated on silicon substrate using vapor transport. Two morphologies, bell-mouthed and uniform hexagonal microtubes, are obtained from the fabrication process. The ZnO hexagonal microtubes have demonstrated ultraviolet (~ 393 nm) lasing emission under 355 nm optical excitation. It is found that the threshold pump intensity and cavity mode spacing of the microtube lasers are ~ 500 kW/cm² and ~ 0.7 nm, respectively. The lasing characteristics of the microtube lasers are also investigated. It is shown that high threshold pump intensity of the microtube lasers is due to the high radiation loss arising from the hollow hexagonal structure near the prismatic facets. [DOI: 10.1143/JJAP.43.5273]

KEYWORDS: lasers, ultraviolet emission, laser resonators, zinc oxide, vapor transport

1. Introduction

Orbital angular momentum, which can be generated by Laguerre–Gaussian beams with a far field pattern of a doughnut shape and an on-axis phase singularity, has been applied to tweeze microscopic particles.¹⁾ This type of doughnut beam can also be generated by applying phase mask modulation,²⁾ direct generation from laser cavity,³⁾ using hollow optical fiber⁴⁾ and computer-generated hologram.⁵⁾ However, the available methods to generate doughnut beams require external lasing source and this increases the complexity of the systems. If an active tubular structure can be formed, a new type of lasing source with output beam similar to a doughnut ring beam can be obtained. Hence, simple and compact active optical tweezers can be realized by using lasing materials with tubular structure.

One-dimensional tubular structures from semiconductor oxides such as TiO₂, SiO₂, Ga₂O₃, In₂O₃, and VO_x have been successfully synthesized⁶⁾ but none of these semiconductor oxides has exhibited strong photoluminescence at room temperature. Recently, ZnO nanorods have been fabricated using vapor transport and strong stimulated emission has been observed under optical excitation.⁷⁾ Hence, if tubular structure of ZnO can be fabricated with the appropriate dimension, it is possible to realize active optical tweezers.

In this paper, the lasing characteristics of ZnO hexagonal microtubes are investigated and the possibility to use ZnO hexagonal microtubes as the active optical tweezers is discussed. This paper is organized as follows: In §2, vapor transport method which is used to fabricate ZnO hexagonal microtubes is described and ultraviolet stimulated emission of the microtube lasers under optical excitation is investigated. Furthermore, ZnO hexagonal microrods with size similar to that of the microtubes have been fabricated and the corresponding lasing characteristics are also being studied. In §3, a theoretical study on the threshold pump intensity of microrod and microtube lasers is made. The reason for a higher threshold pump intensity of microtube lasers is also being investigated. The possibility of using ZnO hexagonal microtube lasers to realize active optical tweezers is also investigated. Discussion and conclusion are given in section 4.

2. Experimental Study

2.1 Fabrication of ZnO hexagonal microtube lasers

The ZnO hexagonal microtubes are grown on silicon (Si) substrate using vapor transport method.⁸⁾ A copper grid, which is often used as the sample holder for transmission electron microscopy, is being used to cover the Si substrate to act as the catalyst. The microtubes are epitaxially grown by heating the mixture of high purity ZnO (99.999%) and graphite powders in air. The X-ray diffraction data has shown that the deposited sample has hexagonal ZnO structure (*c*- and *a*-plane lattice constants equal to 3.250 Å and 5.207 Å, respectively) with (0002) orientation. It is shown by X-ray photoelectron spectroscopy that there is a small amount of Cu (<0.1%) inside the sample. Figure 1 shows the scanning electron microscopic (SEM) images of the ZnO hexagonal microtubes. It clearly shows the prismatic facets of the microtubes can provide optical feedback to achieve stimulated emission. It is estimated that the mean (standard deviation) of the diagonal size of the hexagon and the cavity length of the microtubes are about ~ 12 μm (~ 4 μm) and ~ 50 μm (~ 7 μm), respectively. It is also illustrated in figure 1 that there are two types of ZnO hexagonal microtubes grown on the copper grids: hexagonal bell-mouthed and hexagonal uniform microtubes. The ‘bell-like’ microtubes are mainly presented at the center of the radial array and the ‘uniform’ hexagonal microtubes predominantly appeared around the sidewalls. It is noted that about two-third of the ZnO hexagonal microtubes have inner sidewalls, which composed of nesting layered structure with a perfect hexagonal profile [i.e., see Figure 1(b) and 1(d)]. It is estimated that the diagonal size of the smallest inner hexagon is about one-fifth to that of the outer hexagon of the microtubes.

The vapor-liquid-solid mechanism can be used to explain the formation of ZnO hexagonal microtubes on the Si substrate.⁸⁾ Carbon and its resultant reaction with oxygen, carbon monoxide, acted as reduction agents during formation of ZnO microtubes. ZnO powders were reduced to zinc or its sub-oxide (ZnO_x) with low melting point. The Zn and ZnO_x vapor transferred to low temperature region to form liquid micro-droplets were then recombined with oxygen to form micro-structural ZnO on the substrate. The formation of the hexagonal ZnO microtube is in consistent with the principle of the growth kinetics because both Zn and ZnO

*Corresponding author. E-mail address: esfyu@ntu.edu.sg

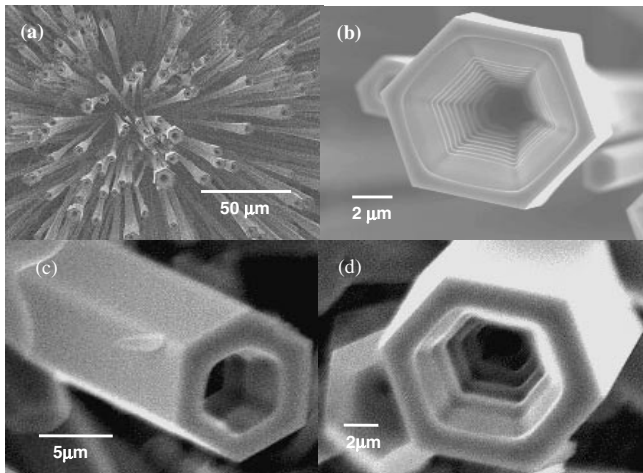


Fig. 1. SEM images of the microtubes: (a) a radial array, (b) enlarged bell-mouthed microtube with nesting layers, (c) enlarged normal hexagonal microtube and (d) enlarged normal hexagonal microtube with nesting layers.

have hexagonal structures. The copper acted as a catalyzing template for Zn and ZnO_x to condensate.⁹⁾ The melting points of Zn and ZnO are 419°C and 1975°C respectively and the boiling point of Zn is 907°C. So the as-grown product might have a Zn cap on top or even a Zn–ZnO coaxial structure as what have been reported by other researchers.¹⁰⁾ In the beginning of the microtube growth, there were plenty of Zn vapors. With the progress of the growth, Zn vapor became less and less because of the limited zinc in the source. The Zn cap on top of the microtube might be evaporated with a typical growth temperature of about 850°C to 900°C. This formation of bell-mouthed microtube observed is possibly due to the stress in the growth process that forced the tube to become a bell. Furthermore, the tubular structures could only be formed with copper grid on Si substrate.

2.2 Lasing characteristics of ZnO hexagonal microtube lasers

The emission spectra of the ZnO microtubes can be excited by a frequency tripled (355 nm) Nd:YAG laser at pulsed operation (6 ns FWHM, 10 Hz). The pump beam is illuminated on the ZnO microtubes at an incident angle of 60°C–70°C to the surface of the Si substrate. The emission light is collected in the direction normal to the surface of the substrate so that only light emitted from the prismatic facets will be detected. Figure 2 plots the light–light curve of the ZnO microtube lasers at room temperature. The corresponding emission spectra at various excitation intensities are also shown in the figure. It is observed that a kink (indicated by an arrow) appears in the light–light curve. At low excitation intensities ($<100 \text{ kW/cm}^2$), a single broad spontaneous emission peak (at ‘A’ with FWHM of $\sim 15 \text{ nm}$) is observed. As the pump power increases at the kink ($\sim 500 \text{ kW/cm}^2$, ‘B’), the envelop of the emission spectrum is narrowed and several sharp peaks emerged in the emission spectrum. The kink is considered as the threshold of the microtube lasers because the emission intensity increases rapidly with the pump intensity and the linewidth of the sharp peaks reduces down to $\sim 0.3 \text{ nm}$. It is observed that the spacing between the

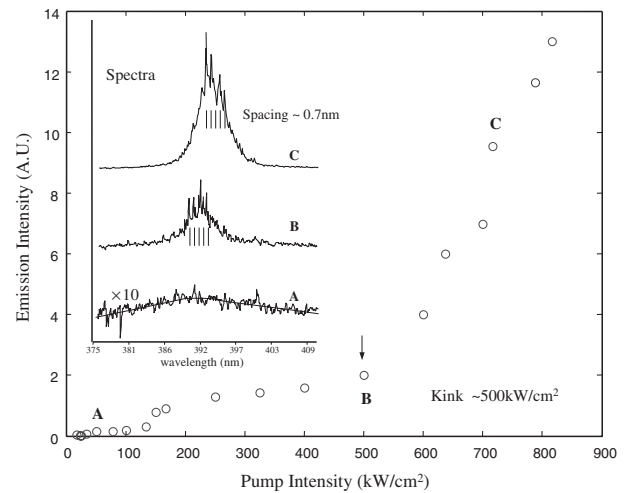


Fig. 2. Light–light curve of the ZnO hexagonal microtube lasers at room temperature under optical pulses excitation. The corresponding emission spectra for various excitation intensities (A, B, and C) are also inserted in the figure. The arrow indicated the position of the threshold on the light–light curve.

sharp peaks is $\sim 0.7 \text{ nm}$ and is roughly unchanged at higher pump intensities (‘C’). It is believed that the electron-hole plasma (EHP) stimulated recombination is the dominant mechanism in the lasing spectra of the microtube laser because the threshold pump intensity is very high when compared to the reported values.¹¹⁾ In the ZnO microcrystallite thin films, the excitation intensity for the EHP stimulated recombination is $\sim 110 \text{ kW/cm}^2$.⁷⁾

It must be noted that random lasing action will not be supported in ZnO hexagonal microtubes because the separation between microtubes are much longer than the scattering mean free path.¹²⁾ In addition, the ZnO powder crystal if any on the surface of the substrate will not lead to random lasing action because the pump intensity is strongly absorbed by the long ZnO microtubes before it can reach the substrate surface. Hence, we attribute the lasing characteristics of the ZnO hexagonal microtubes to optical feedback from the prismatic facets and interfaces between Si substrate and ZnO microtubes so that the microtubes support Fabry Perot (FP) modes. The irregular shape of the lasing spectra is in fact due to the incoherent superposition of the emission from a series of microtube lasers with random variation of cavity length. However, the most distinct lasing modes in the lasing spectra have roughly equal separation of $\Delta\lambda \sim 0.7 \text{ nm}$. This indicates that large population of the microtubes have an average cavity length of L . L can be estimated by using $\Delta\lambda = \lambda_0^2/2n_{\text{eff}}L$, where n_{eff} is the effective refractive index of the microtubes and λ_0 ($= 390 \text{ nm}$) is the lasing wavelength. If n_{eff} is assumed to be 2.1 (same as the refractive index of ZnO), it is found that $L \sim 52 \mu\text{m}$, which is close to the expected average cavity length of the microtube lasers.

2.3 Lasing characteristics of ZnO microrod lasers

Figure 3 shows the SEM image of the ZnO hexagonal microrods grown on Si substrate. The microrods are also grown by vapor transport with similar processing parameters as in the microtubes except that the copper grid is not used during the growth process. It can be shown that the size of

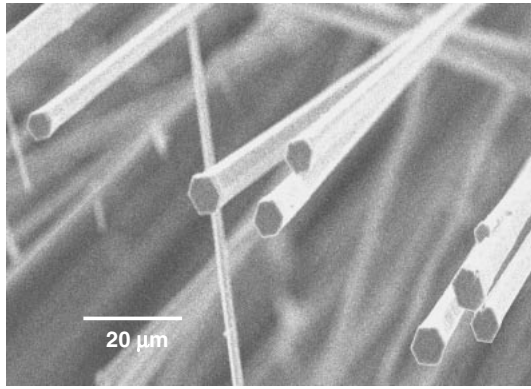


Fig. 3. SEM images of the microrods.

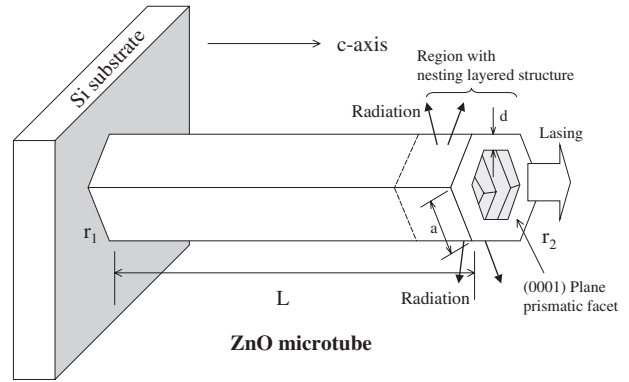


Fig. 5. Schematic of the ZnO hexagonal microtube grown on silicon substrate.

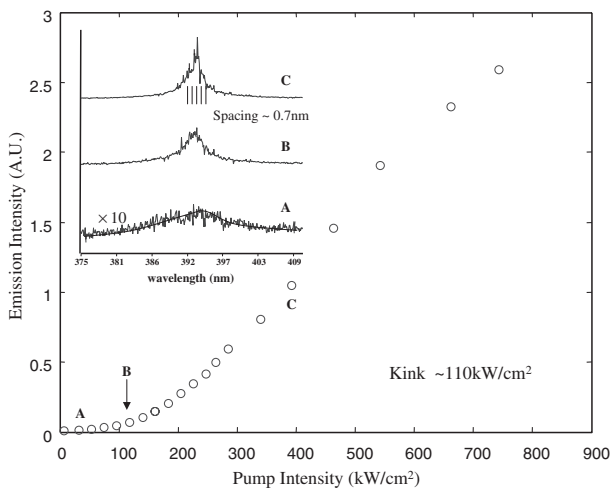


Fig. 4. Light-light curve of the ZnO hexagonal microrod lasers at room temperature under optical pulses excitation. The corresponding emission spectra for various excitation intensities (A, B, and C) are also inserted in the figure. The arrow indicated the position of the threshold on the light-light curve.

the ZnO hexagonal microrods is similar to that of the microtubes except there is no hole inside the microrods. It is believed that the clear prismatic facets and the interface between the microrods and Si substrate provide optical feedback to sustain stimulated emission.

Figure 4 plots the light-light curve and the inset is the optical spectra at various pump intensity of the ZnO hexagonal microrod lasers. It is shown that the lasing spectra also exhibit irregularly in shape but the most distinct lasing modes still have roughly equal separation so that the average cavity length of the microrods can be estimated. It is observed that the approximated spectra separation of modes is ~ 0.7 nm. Hence, it is believed that the average cavity length of both microrod and microtube lasers is similar. However, the threshold pumped intensity of the microrod lasers (~ 110 kW/cm²) is about 5 times lesser than that of the microtube lasers (~ 500 kW/cm²). This implies that the hollow hexagonal structure of microtube lasers significantly increases the corresponding total cavity loss.

3. Theoretical Investigation

Figure 5 shows a schematic of the ultraviolet prismatic ZnO hexagonal microtube laser to be investigated. It is

assumed that the microtubes are grown in the direction perpendicular to the surface of the Si substrate. In the figure, 'L' is the length, 'a' is the width and 'd' is the sidewall thickness of the microtube. r_1 and r_2 are the field reflectivities of the prismatic facet and the interface between Si substrate and ZnO microtube, respectively. The shape of the ZnO hexagonal microrod lasers used in our analysis is similar to that shown in Fig. 5 except the prismatic facets have no hexagonal holes.

3.1 Threshold Characteristics of ZnO Hexagonal Micro-rod lasers

In ZnO hexagonal microrods, it is believed that the optical field is strongly confined inside the microrods in the direction parallel to the plane of Si substrate. Figure 6 shows the schematic cross section of a hexagonal microrod. It is noted that the critical angle, θ_c , (minimum angle to obtain total internal reflection) between the sidewalls of the ZnO hexagonal waveguide and air interface is about 28.43° . Hence, the ray tracing analysis shows that standing wave can be established within the hexagonal structure by following the six-bounce closed loop trajectories with an incident angle of 60° . This ray tracing analysis is valid provided that the diameter of the microrod is much longer than the lasing wavelength. As a result, light is strongly confined inside the hexagonal structure and no radiation of light will be allowed from the sidewalls of the microrods. Therefore, lasing modes can only be supported by optical feedback between the

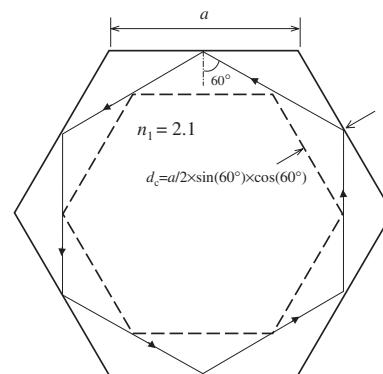


Fig. 6. Schematic cross-section of the ZnO hexagonal microrod. The requirement of total internal reflection inside the microrod is also indicated by the arrows.

prismatic facet and the interface between Si substrate and microrod. Light will emit from the prismatic facet and the corresponding total facet loss, α_F , can be expressed as¹³⁾

$$\alpha_F = \frac{1}{L} \ln \left(\frac{1}{|r_1 r_2|} \right). \quad (1)$$

Refractive index of Si is about 3.44 at 390 nm so that $r_1 \sim 0.24$ and $r_2 \sim 0.35$ (perfect reflection from a dielectric interface). Hence, it can be shown that $\alpha_F \sim 0.5 \times 10^3 \text{ cm}^{-1}$ for $L = 50 \mu\text{m}$.

3.2 Threshold Characteristics of ZnO Hexagonal Microtube lasers

In ZnO hexagonal microtube lasers, light may not be confined inside the microtube if $d < d_c$, where d_c is the critical thickness or the minimum thickness of d to sustain total internal reflection. Refer to Fig. 6, d_c can be deduced from ray tracing analysis and can be written as

$$d_c = \frac{\sqrt{3}}{8} a + \frac{\lambda_0}{2}. \quad (2)$$

From (2), if $a = 6 \mu\text{m}$, it can be shown that $d_c \sim 1.5 \mu\text{m}$. Therefore, it is expected that light will still be guided inside the lower portion (near the Si substrate) of the microtubes as $d > d_c$ is normally found. On the other hand, due to the nesting layered structure near the prismatic facets, the microtubes may have a much wider hexagonal hole such that $d < d_c$ may occur. As a result, the guidance of the optical field parallel to the plate of Si substrate may cease near the prismatic facets and the radiation of light from the sidewalls may allow.

Radiation loss near the prismatic facets can be estimated by studying the modal characteristics in the direction parallel to the prismatic facets of the ZnO hexagonal microtubes. Figure 7 shows the cross section of the microtube, which can be assumed to be a hexagonal slab waveguide oscillator with ZnO of refractive index n_1 as the core region and air of refractive index n_{air} as the cladding regions. The modal characteristics of the hexagonal slab waveguide oscillator can be investigated through the study of the loss and phase of the corresponding tilted slab waveguide. In the diagram, it

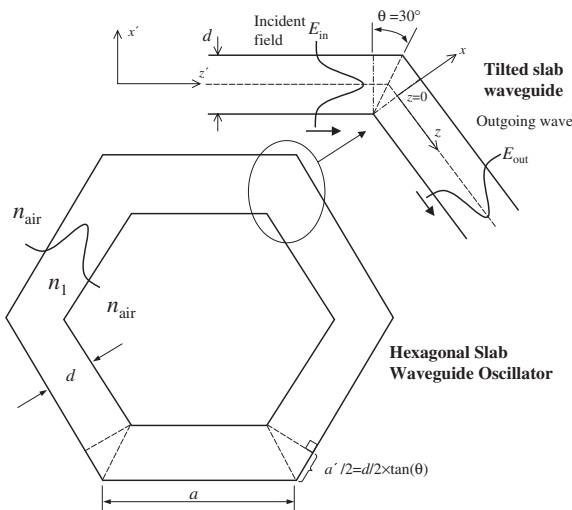


Fig. 7. Schematic cross-section of the ZnO hexagonal microtube.

is assumed that the incident field excites the outgoing wave inside the tilted waveguide. The incident field, E_{in} , and the outgoing field, E_{out} , can be written as

$$E_{\text{in}}(x', z') = f_m(x') \exp(-j\beta_m z'), \quad (3a)$$

$$E_{\text{out}}(x, z) = f_m(x) \exp(-j\beta_m z), \quad (3b)$$

where $j = \sqrt{-1}$, f_m , whose base system consists of sine and cosine functions, is the normalized m th order TE mode and β_m is the corresponding propagation coefficient. The coordinate system (x, z) and (x', z') can be related by

$$x' = x \cos(2\theta) - z \sin(2\theta), \quad (4a)$$

$$z' = x \sin(2\theta) + z \cos(2\theta). \quad (4b)$$

Hence, E_{in} can be expressed in (x, z) coordinate system as shown below:

$$E_{\text{in}}(x, z) = f_m(x \cos(2\theta) - z \sin(2\theta)) \times \exp(-j\beta_m(x \sin(2\theta) + z \cos(2\theta))). \quad (5)$$

From eqs. (3) and (5), if the two fields were perfectly aligned (i.e., $\theta = 0$), their overlap integral or transmission coefficient would be unity. However, the tilt causes radiation loss due to the misalignment of the phase fronts between the incident and outgoing waves. The transmission coefficient, t_m , through the tilted section of the slab waveguide can be obtained by calculating the overlap integral of E_{in} and E_{out} at $z = 0$, that is¹⁴⁾

$$t_m = \int_{-\infty}^{\infty} E_{\text{in}}^*(x) E_{\text{out}}(x) dx = \int_{-\infty}^{\infty} f_m(x) f_m(x \cos(2\theta)) e^{j\beta_m \sin(2\theta)x} dx, \quad (6)$$

where * denotes complex conjugation and orthogonal behavior between guided modes is assumed.

In order to obtain the confinement of light inside the hexagonal slab waveguide oscillator, the following round-trip conditions should be satisfied. This is

$$1 = |t_m|^6 \exp([3g + j6\beta_m]a') \exp(j6\phi_m), \quad (7)$$

where it is assumed that $t_m = |t_m| \exp(j\phi_m)$, ϕ_m is the phase of t_m , g is the gain and $a' = a - d \tan(\theta)$. The real and imaginary parts of eq. (7) correspond to the round-trip gain and phase conditions, respectively, of the hexagonal slab waveguide oscillator. The round-trip gain and phase conditions can be written as

$$g = \frac{1}{\Gamma_m a'} \ln \left(\frac{1}{|t_m|^2} \right) \equiv \alpha_R, \quad (8a)$$

$$\frac{1}{3} \eta \pi = \beta_m a' + \phi_m, \quad (8b)$$

where $\eta = 0, 1, 2, \dots$, Γ_m is the confinement factor of the guided mode inside the slab waveguide and α_R is defined as the radiation loss of the ZnO hexagonal microtube lasers. From eq. (8b), it is noted that the propagation constant, β_m , will be slightly modified by the round-trip phase condition of the hexagonal slab waveguide oscillator. However, this effect will only have a small influence on the value of $|t_m|^2$. Figure 8a plots $|t_m|^2$ versus d of the first eight TE modes (i.e., $m = 0, 1, \dots, 7$) that are supported inside the tilted slab waveguide for the given range of d (i.e., the mode cutoff values of d for modes $m = 5, 6$, and 7 are roughly equal to $0.52, 0.63$ and $0.74 \mu\text{m}$, respectively). The slab waveguide is

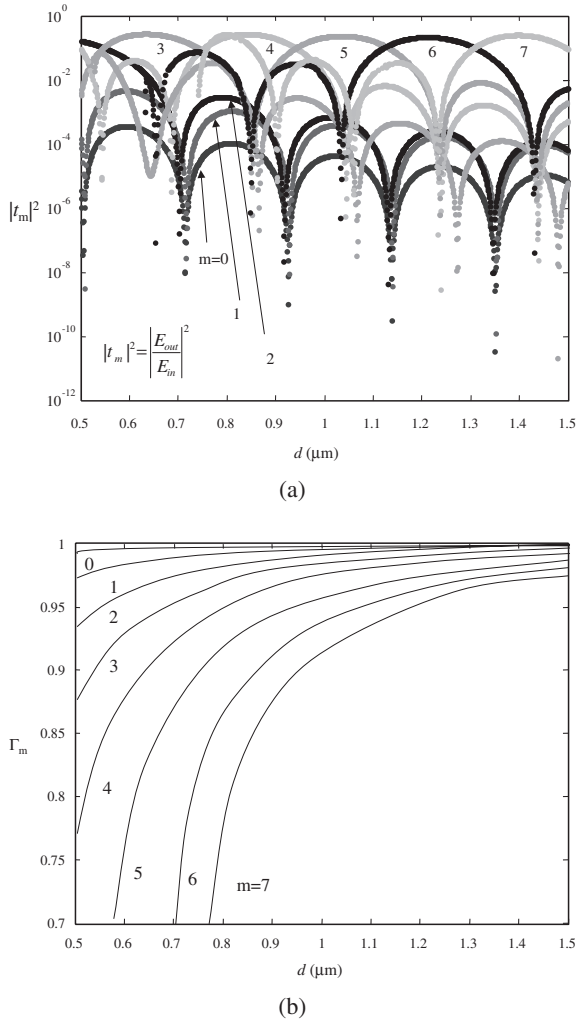


Fig. 8. Plots of (a) $|t_m|^2$ versus d and (b) Γ_m versus d for the first eight TE guided modes inside the slab waveguide.

assumed to have $n_1 = 2.1$, $n_{\text{air}} = 1.0$ and the optical modes have free space wavelength $\lambda_0 = 393 \text{ nm}$. In the figure, it is observed that the value of $|t_m|^2$ of all the guided modes have local minimum and maximum over the range of d . This is because of the constructive or destructive interference between the outgoing and incident fields at different value of d . In addition, there are at most two modes that will be guided inside the slab waveguide for a given value of d (e.g. mode 6 and 7 are supported and propagated inside the slab waveguide with $d \sim 1.31 \mu\text{m}$). The plot of Γ_m versus d for the corresponding TE modes is shown in Fig. 8(b). It is expected that the increase in d increases the value of Γ_m as the optical confinement of the guided modes increases with the value of d . It must be noted that although the mean value of a is assumed to be $6 \mu\text{m}$, the value of d in each microtube may vary along the c -axis due to the nesting layered structure. For each microtube, the value of d may vary from $0.5 \mu\text{m}$ to more than $1.5 \mu\text{m}$ so that the average value of $|t_m|^2$ can only be estimated from eq. (6). It can be shown that for the microtubes with $a \sim 6 \mu\text{m}$, the average value of $\ln(1/|t_m|^2)$ for all the guided modes inside the nesting layered structure (i.e., $0.5 \mu\text{m} \leq d \leq 1.5 \mu\text{m}$) can be ~ 1.2 . In the calculation, it is assumed that the diagonal size of the inner hexagon is reduced to one-fifth to that of the outer

hexagon over a distance $\sim 10 \mu\text{m}$ along the c -axis of the microtubes. Hence, the average radiation loss of the nesting layered structure can be obtained from eq. (8a) and is given by $\alpha_R \sim 2.2 \times 10^3 \text{ cm}^{-1}$.

Apart from the radiation loss, light is also emitted from the prismatic facets as well as the interfaces between the Si substrate and ZnO microtubes and the corresponding cavity loss can be obtained from eq. (1). This approximation is possible because the propagation modes along the c -axis are orthogonally orientated in a direction parallel to the Si substrate. Therefore, the total loss of the microtube lasers is the addition of 1) loss from the prismatic facets, α_F and 2) radiation loss from the sidewalls of the microtubes, α_R , and that is equal to $\alpha_F + \alpha_R = (0.5 + 2.2) \times 10^3 \text{ cm}^{-1}$. Obviously, the extra radiation loss of the microtube lasers when compared with the microrod lasers is due to the hollow hexagonal structure.

From the above estimation, the total loss of the microtube lasers is about 5 times higher than that of microrod lasers (i.e., $(\alpha_F + \alpha_R)/\alpha_F \sim 5$). This may be the reason why the threshold pump intensity of the microtube lasers is about 5 times higher than that of the microrod lasers. The relation between threshold pump intensity and total loss can be deduced by the following rate equations:

$$\frac{\partial N}{\partial t} = \frac{\alpha_{\text{abs}}}{\hbar\nu} P - \frac{N}{\tau_N} - R_{\text{st}}(N), \quad (9a)$$

$$\frac{\partial S}{\partial t} = \nu_g (g - \alpha_{\text{total}}) S + R_{\text{sp}}, \quad (9b)$$

where S is the photon density, N is the carrier concentration, P is the pump intensity (W/cm^2), α_{abs} is the absorption coefficient (cm^{-1}), ν is the frequency, ν_g is the group velocity, τ_N is the carrier lifetime, α_{total} is the total cavity loss, g is the optical gain, R_{sp} is the spontaneous emission rate and R_{st} is the stimulated recombination rate. Since EHP stimulated recombination is dominant in the emission process, it is reasonable to approximate $g = a_N(N - N_{\text{EHP}})$, where a_N is the gain coefficient and N_{EHP} is the threshold carrier concentration for EHP recombination. From eq. (9), it can be shown that the steady state relationship between α_{total} and P at threshold is given by

$$\frac{\alpha_{\text{total}}}{a_N} + N_{\text{EHP}} = \frac{\tau_N \alpha_{\text{abs}}}{\hbar\nu} P. \quad (10)$$

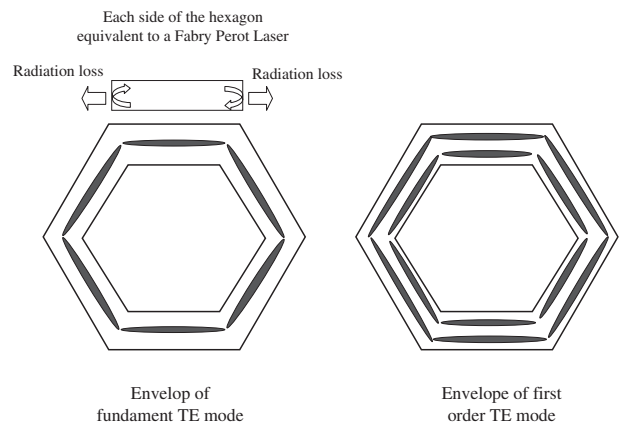


Fig. 9. The near field optical profile of the ZnO hexagonal microtube lasers.

In the derivation, it is assumed that $R_{st} = 0$ in eq. (9a) as $S = 0$ at threshold and $R_{sp} = 0$ in eq. (9b). If the threshold pump intensity and total cavity loss of the microtubes (microrods) are assumed to be P_T (P_F) and $\alpha_F + \alpha_R$ (α_F), respectively, then it can be shown that

$$\frac{\alpha_T - \alpha_F}{a_N} = \frac{\tau_N \alpha_{abs}}{\hbar \nu} (P_T - P_F), \quad (11)$$

where $\alpha_T = \alpha_F + \alpha_R$. From the measurement, it is noted that the threshold pump intensities for the microtubes, P_T , and microrods, P_F , are 500 kW/cm^2 and 110 kW/cm^2 , respectively so that $P_T \sim 5P_F$ is roughly agreed. Substitutes $P_T \sim 5P_F$ into eq. (11), it can be shown that $\alpha_T \sim 5\alpha_F$. In fact, our estimation has found that the values of $(\alpha_F + \alpha_R)$ and α_F , are $(0.5 + 2.2) \times 10^3 \text{ cm}^{-1}$ and $0.5 \times 10^3 \text{ cm}^{-1}$, respectively so that $\alpha_T \sim 5\alpha_F$ is in agreement with eq. (11). Hence, we have proved that the increase in threshold pump intensity in microtube lasers is due to the hollow hexagonal structure as the hollow hexagonal structure induces radiation loss.

3.3 Modal characteristics of the ZnO hexagonal microtubes at the prismatic facets

The radiation modes at the prismatic facets of the microtube lasers can be calculated from eq. (3). Considering one side of the hexagonal microtubes, the profile of the modes, $E(x, z)$, can be expressed as

$$E(x, z) = f_m(x) (Ae^{-j\beta_m z} + Be^{+j\beta_m z}) = Af_m(x) \cos(\beta_m z), \quad (12)$$

where A and B are the amplitudes of the forward and reverse fields and they should have the same magnitude due to the symmetric property of the hexagonal structure. For d equals to $1.0 \mu\text{m}$, β_0 of the fundamental TE mode is about $33.7 \mu\text{m}^{-1}$. The magnitude of $1/\beta_0$ is much shorter than that of a ($\sim 6 \mu\text{m}$) so that the radiation modes are similar to the longitudinal modes inside a FP cavity with low facet reflectivities and hence the corresponding slow variation envelop of the propagation fields should be quite uniform over the sides of the hexagonal microtubes. Figure 9 sketches the modal characteristics of the prismatic facets of a hexagonal microtube laser for the fundamental and first order TE modes for $d < 0.5 \mu\text{m}$. As we can see, the light intensity is quite uniform along the side of the hexagonal structure but the intensity goes dim (due to radiation of light) at the corner of the hexagon. Nevertheless, the output beam from the prismatic facets has the shape similar to a doughnut ring, which can be used as optical tweezers.

4. Discussion and Conclusion

During the growth process of ZnO hexagonal microtubes by vapor transport, two morphologies (bell-mouthed and uniform hexagonal microtubes) can be obtained simultaneously. It is noted that the formation of both morphologies is dependent on the use of ZnO mixtures and copper catalyst. However, it is still not possible to control the yield rate of the required morphology. On the other hand, both morphologies can be used to realize optical tweezers but the use of the bell-mouthed microtubes is more suitable for this particular applications. This is because bell-mouthed microtubes have shorter nesting layered structure (thinner sidewalls) so that the corresponding threshold pump intensity (quality of optical fields at the prismatic facets) is lower

(better) than that of the uniform one. Therefore, it is necessary to optimize the fabrication process to increase the yield rate of the bell-mouthed microtubes on the Si substrate.

Although irregular shape (due to incoherent superposition of emission spectra from a series of FP cavities with random variation of cavity length) of lasing spectra from the ZnO hexagonal microtube lasers is observed (in Fig. 2), the roughly equal spacing of the most distinct lasing modes indicates that the microtube lasers sustain FP modes. Furthermore, the emission spectra are collected by an objective lens in the direction perpendicular to the surface of the prismatic facets so that light radiating from the sidewalls of the microtubes will not appear from the lasing spectra. Hence, it is proved that the ZnO hexagonal microtube lasers sustain FP modes due to the optical feedback from the prismatic facet and interface between Si substrate and ZnO microtube.

In conclusion, the prismatic ZnO hexagonal microtubes have been fabricated using vapor transport. It is demonstrated that the ZnO microtubes can only be grown epitaxially on the substrate using copper grid as the catalyst. Stimulated emission at $\sim 393 \text{ nm}$ is observed in the ZnO microtube lasers under the 355 nm optical pulse excitation. It is found that the threshold pump intensity and spacing of the FP modes are $\sim 500 \text{ kW/cm}^2$ and $\sim 0.7 \text{ nm}$, respectively. Radiation loss and modal characteristics of the ZnO hexagonal microtubes are studied by investigating the resonant conditions of hexagonal slab waveguide oscillator. It is found that the high threshold pump intensity of microtube lasers is due to the presence of the hollow hexagonal structure, which induces high radiation loss near the prismatic facets. In addition, it is shown that the output beam from the prismatic facets has a shape similar to a doughnut ring so that ZnO hexagonal microtube lasers can be used to realize active optical tweezers.

Acknowledgement

This project is supported by A*STAR Grant project number 022-101-0033, Nippon Sheet Glass Foundation and NTU/RGM grant no: RGM 18/02.

- 1) L. Allen, M. W. Beijersbergen, R. J. C. Spreeuw and J. P. Woerdman: Phys. Rev. A **45** (1992) 8185.
- 2) M. W. Beijersbergen, R. P. C. Coerwinkel, M. Kristensen and J. P. Woerdman: Opt. Commun. **112** (1994) 321.
- 3) Y. I. Shin, K. Kim, J. A. Kim, H. R. Noh, W. Jhe, K. Oh and U. C. Paek: Opt. Lett. **26** (2001) 119.
- 4) K. T. Gahagan and G. A. Swartzlander: Opt. Lett. **21** (1996) 827.
- 5) Chr. Tamm and C. O. Weiss: J. Opt. Soc. Am. B **7** (1990) 1034.
- 6) J. Q. Hu and Y. Bando: Appl. Phys. Lett. **82** (2003) 1401.
- 7) Z. K. Tang, G. K. L. Wong, P. Yu, M. Kawaski, A. Ohtomo, H. Koinuma and Y. Segawa: Appl. Phys. Lett. **72** (1998) 3270.
- 8) M. H. Huang, Y. Wu, H. Feick, N. Tran, E. Weber and P. Yang: Adv. Mater. **13** (2001) 113.
- 9) S. Y. Li, C. Y. Lee and T. Y. Tseng: J. Cryst. Growth **247** (2003) 357.
- 10) J. J. Wu, S. C. Liu, C. T. Wu, K. H. Chen and L. C. Chen: Appl. Phys. Lett. **81** (2002) 1312.
- 11) M. H. Huang, S. Mao, H. Feick, H. Q. Yan, Y. Y. Wu, H. N. Kind, E. Weber, R. Russo and P. D. Yang: Science **292** (2001) 1897.
- 12) H. Cao, Y. G. Zhao, S. T. Ho, E. W. Seelig, Q. H. Wang and R. P. H. Chang: Phys. Rev. Lett. **82** (1999) 2278.
- 13) A. Yariv: *Optical Electronics* (Holt-Saunders International Editions, New York, 1985) 3rd ed., Chap. 6.
- 14) D. Marcuse: J. Lightwave Technol. **2** (1989) 336.